

MICRO-MECHANICAL STUDIES ON PURE AND Ni DOPED ZnS NANOSTRUCTURED CRYSTALS

ARFAT FIRDOUS^{a,b}, TANVEER RASOOL^c, G.N.DAR^d, M.M.AHMAD^a

^a*Department of Physics, National Institute of Technology, Hazratbal, Srinagar - 190006, J & K, India*

^b*Department of higher education, Dept. of physics, GDC, Handwara, J&K, India*

^c*Department of Chemical Engineering, National Institute of Technology, , Srinagar-190006, India*

^d*Department of Physics, University of Kashmir, J&K-190006, India.*

The results obtained on indentation induced Vicker's microhardness and fracture toughness studies in the load range of 0.049 to 3N on pure and Ni modified ZnS nanocrystals, are presented. The load dependence of Vicker's hardness (VHN) is explained on the basis of Hays and Kendall's law. Load independent values of VHN are worked out by application of Hays's and Kendall's law for pure and Ni modified compositions of ZnS nanocrystals and the same is shown to increase with the increase in Ni substitution. Fracture toughness, internal stress and brittleness index for these samples have also been calculated using microindentation technique.

(Received September 15, 2010; accepted October 15, 2010)

Keywords: Nano-material ;Doping, Microhardness, Fracture toughness, Internal stress

1. Introduction

Zinc sulfide is an important type of II- VI group semiconductor with its wide band gap energy of 3.67 eV at room temperature is particularly suitable for use as luminescent host materials for a very large variety of dopants. Doped semiconductor nanocrystals have received a considerable effort since the initial research work on the luminescence properties of Mn²⁺ ions doped ZnS nanocrystals [1]. Doped semiconductor nanocrystals have attracted extensive research interests in the recent years due to their unique optical properties and potential applications [2]. Numerous researchers have investigated the structural and luminescence properties of doped phosphor nanoparticles [3- 5] especially Mn²⁺ doped ZnS nanocrystals [6-10]. The doping ions act as recombination centers for the excited electron- hole pairs and result in strong and characteristic luminescence. Synthesis and luminescence properties of doped ZnS nanocrystals have been extensively studied. However, with the decrease of particle size, extremely high surface to volume ratio causes the surface states to act as luminescent quenching centers. Hence the passivation of surface is of crucial importance for the applications of this type of luminescent semiconductor nanomaterials. In optoelectronics, it finds use as light emitting diode, reflector, dielectric filter and window material. Among the family of II-VI semiconductors, ZnS, CdS, ZnO, CdTe, etc. are the foremost candidates because of their favorable electronic and optical properties for optoelectronic applications. ZnS has been used for the cathode ray tube, the field emission display, and the scintillator, as one of the most frequently used phosphors. In addition, a ZnS crystal laser has been produced using streamer excitation, and thin films of ZnS can be used as an active emitting material in such a device, termed the hot electron cold cathode. These doped ZnS semiconductor materials have a wide range of applications in electroluminescence devices, phosphors, light emitting displays, and optical sensors. Accordingly, study of luminescence properties of ZnS has received special attention. In addition to the blue luminescence of ZnS host, emission in different visible bands related to various dopants has been reported [7-10]. Of all the

materials investigated, ZnS is a material that has fascinated researchers with its variety of morphologies and range of promising device application [11-15]. Pure and Ni doped ZnS nanocrystals prepared through chemical route are found to have cubic crystal structure with the diffraction peaks coming from (111), (220), and (311) planes. On modifying pure ZnS by Ni optical band gap decrease. The electrical measurements carried out using two-probe technique reveal semiconducting nature of both pure and Ni modified ZnS. The calculations based on VRH model suggest the increase in conductivity of Ni modified ZnS due to induced disordered localization. These results are already reported by the author [16]. The microhardness is a mechanical parameter which is strongly related to the structure and composition of the crystalline solids. Mechanical properties of a material are intimately connected with the physical and electrical properties as they determine the strength and lasting characteristics of a material in operation. Among several mechanical properties hardness determination is an interesting one. Micromechanical hardness of a material is the measure of resistance which it offers to permanent deformation under the action of applied load [17]. Micromechanical hardness is not only simply a mechanical property that is routinely measured but also an important parameter of a material which is related with the internal structure of the material. Microhardness testing is one of the best methods for understanding the mechanical properties of materials such as elastic constants [18], yield strength, plasticity, hardness anisotropy, creep behaviour and fracture behaviour [19]. In this paper the authors report micromechanical studies of pure and Ni modified ZnS nanocrystals. In the present article, authors report the modifications and changes caused due to doping of Ni ions on mechanical characteristics of ZnS nanocrystals. The mechanical characteristics include studying effect of Ni on variation of hardness and indentation-induced crack propagation leading to determination of the values of fracture toughness and brittleness index.

2. Experimental

Pure and Ni doped ZnS nanoparticles were precipitated from a mixture of zinc acetate and Nickel dichloride with sodium sulfide in aqueous solution. In a typical procedure, aqueous solution of sodium sulfide was added into aqueous solution of zinc acetate and aqueous solution of Nickel dichloride with the molar ratio of Zn:S being 1:1 to obtain white fluid. Then mercaptoethanol (HOCH₂CH₂SH) was added to the above solution, with constant stirring at room temperature. The resulting precipitates were filtered and washed several times with double distilled water and ethanol. Washings were done to remove any organic part or any other impurity from the particles. The as prepared nano material was precalcinated for 12 h at 1000 °C. The precalcinated materials were again ground and calcinated twice at 1300 °C for 24 h, following in between grinding and pelletization for better homogeneity.

The selected smooth as prepared surfaces of the crystal were subjected to the static indentation tests at room temperature using a Vicker's microhardness tester (mhp-100) attached to a large incident light microscope (UHL VMHT MOT GERMANY). Loads ranging from 0.049 to 3N were used for making indentations, keeping time of indentation constant at 10s in all cases. At least five indentation marks were obtained on each face for the same load, the distance between consecutive marks being kept more than three times the diagonal length of the indentation mark. The diagonal lengths of the indentation mark and crack length were measured, using the micrometer eye-piece at a magnification of x500. The microhardness value was calculated using the Equation,

$$H_v = 1.8544P/d^2 \text{ N/m}^2 \quad (1)$$

where k is a geometrical conversion factor for the indenter used and its numerical value depends on the units of P and d. In the case of the Vickers indenter when P is taken in g and d in μm, the geometrical factor k = 1854 and H_v is in VHN (Vickers Hardness Number). However, when P is taken in N and d is in μm, then the geometrical conversion factor is 1854 and hardness is in GN/m². Well-defined cracks were considered for the measurement of the crack length and the average crack length of all such cracks was taken for a particular indentation impression. The crack length

was measured from the centre of the indentation mark up to the tip of the crack. The error in H_v was calculated through the relation

$$\Delta H_v = 1.8544[(\Delta P/Y)^2 + (P\Delta Y/Y^2)^2]^{1/2}$$

where $Y=d^2$, $\Delta Y=2d\Delta d$; ΔP , ΔY and Δd are the experimental errors in P , Y and d respectively. Here the offset in diagonal tip is $< 0.25 \mu\text{m}$ and the load resolution is 0.001 N , the error on P and d were taken less than these values. The error bar fit was carried out through the software Origin 6.0

3. Results and discussion

3.1 Load dependence of hardness:

Fig.1 shows the variation of microhardness with applied load for compositions Pure and Ni doped ZnS nano crystals. The microhardness decreases non-linearly as the applied load increases from 0.049-3N for all compositions.

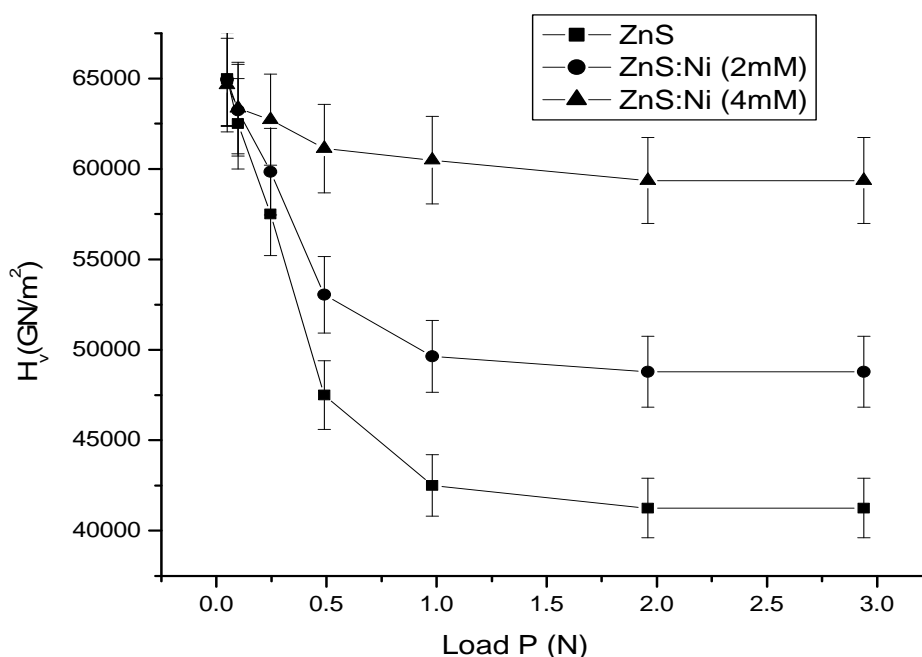


Fig.1. Effect of applied load on Vickers microhardness

It is observed that in doped crystals, the value of Vickers microhardness H_v corresponding to each load increases. This increase in the value of microhardness for doped crystals can be quantitatively explained on the basis of depth penetration of the indenter. Since the indenter penetrates only surface layers at low loads, the effect is more pronounced at these loads. However, as depth penetration increases, the effect of inner layers becomes more and more prominent and ultimately there is no change in the values of hardness with load[19]. This is what happens at loads at 0.8N in this particular case. The relations between load P and diagonal length d is proposed in the literature as follows: Kick's relation [20],

$$P = K_1 d^n \quad (1)$$

where K_1 is the standard hardness constant and n is the Meyer's index which equals 2 for all indenters and for all geometrically similar impressions.

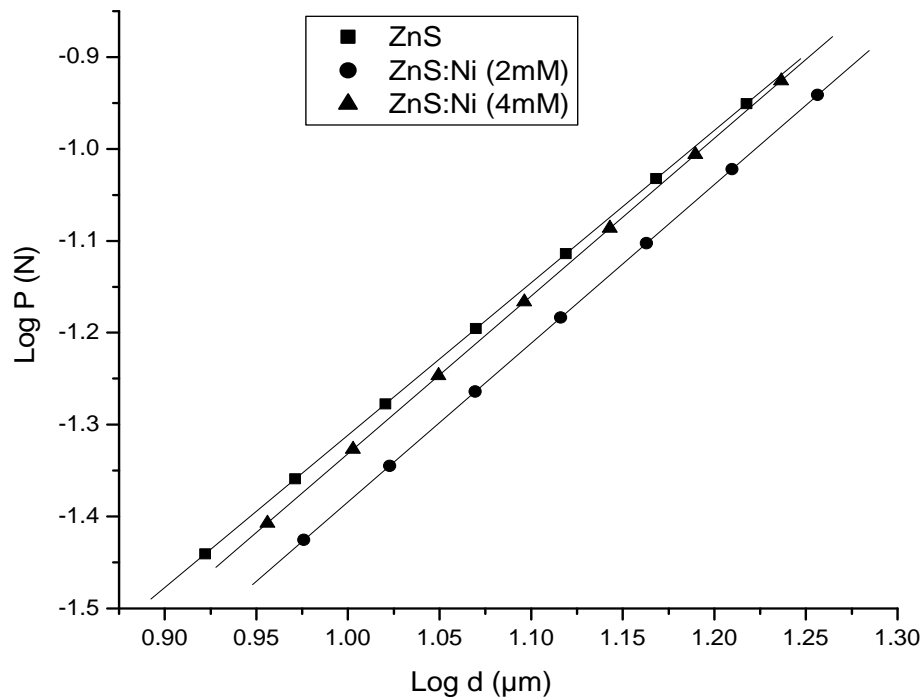


Fig. 2. $\log P$ vs. $\log d$

The equation suggests H_v to be independent of load. That is not true in the present case. The values of n are 1.69, 1.65 and 1.64 for Pure and Ni doped ZnS nano crystals compositions. This supports the concept of Onitsch [21] that for $n < 2$, the microhardness number decreases as the load increases. In low-load regions, the resistance offered by the material may be comparable with the applied load, resulting in a higher value of hardness since indenter penetrates only surface layers. However, at higher loads, the plastic flow of the material may be greater and hence the resistance offered by the material is negligible, thus decreasing the hardness. This type of behaviour is also reported and favoured by several authors [19-20] on the basis of depth penetration of the indenter. Hays and Kendall's [22] relation is:

$$P-W = K_2 d^2 \quad (2)$$

where K_2 is a constant and $n = 2$ is the logarithmic index. It is based on the assumption that as the load is applied to a specimen, it is partially affected by a smaller resistance pressure W , which is a function of the material being tested and represents the minimum applied load to produce an indentation; load less than W not allowing any plastic deformation. In order to evaluate the function W for a particular solution, Eq.'s (1&2) may be subtracted to yield

$$W = K_1 d^n - K_2 d^2 \quad (3)$$

$$\& \quad d^n = K_2 / K_1 d^2 + W / K_1 \quad (4)$$

A plot of $\log P$ against $\log d$ for Pure and Ni doped ZnS nano crystals samples, (Fig. 2) according to Eq. (4) gives the values of n and K_1 . K_2 and W are calculated from a graph between d^n versus d^2 . The values of these constants have been determined by using method of least square

fitting using software Matlab. A plot of $\log(P-W)$ versus $\log d$ as shown in Fig. 3. yields the value of $n=1.99, 1.98, 1.96$, for Pure and Ni doped ZnS nano crystals, thereby suggesting the validity of the theory involving concept of resistance pressure (W) proposed by Hays and Kendall. The data on n, K_1, K_2 and W thus determined and is given in Table 1. The application of Hay and Kendall's law leads to a modified formula of Eq. (1) which gives load independent values of H_v .

$$H_v = 1.8544(P-W)/d^2 \quad (5)$$

Substituting for $(P-W)$ from Eq. (2), we have:

$$H_v = 1.8544K_2 \quad (6)$$

In the light of this equation, the "load independent microhardness values" for Pure and Ni doped ZnS nano crystals crystals are $H_v(x=0) = 1630 \text{ MN/m}^2, H_v(x=0.2) = 2893 \text{ MN/m}^2$ and $H_v(x=0.4) = 3875 \text{ Mn/m}^2$. This clearly shows that microhardness values increase on modifying parent crystals with Ni. One may notice from Fig.1 that H_v has a rapid fall as the load is increased from 0.049 to 1N. Beyond 1N, the microhardness value achieves saturation and becomes load independent. The load independent values thus given are very close to the values calculated on application of Hays and Kendall's law. The load independent values of microhardness is found to increase in Ni substituted crystals.

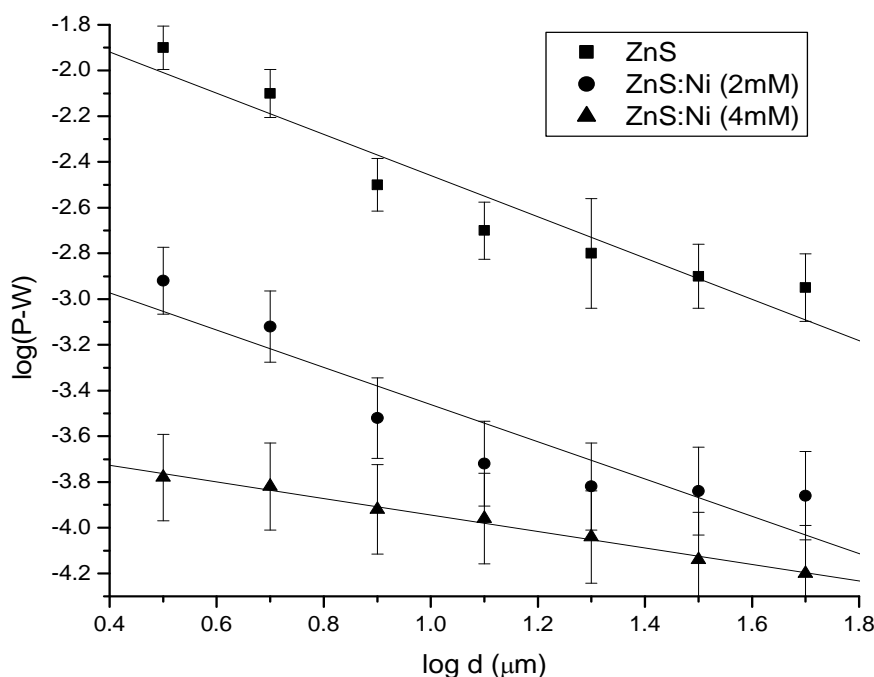


Fig. 3. $\log(P-W)$ vs. $\log d$

3.2 Fracture toughness and brittleness index

The term toughness may be defined as the property of a material by virtue of which it can absorb maximum energy before fracture takes place. The importance of toughness is in the selection of a material where load exceeds the elastic limit or yield point. The indentation impressions are usually seen associated with cracks at almost all loads **on** for Pure and Ni doped ZnS nano crystals crystals. The resistance to fracture indicates the toughness of a material. The cracks developed in a crystal determine the fracture toughness K_{Ic} , which in turn tells us how

fracture stress is applied on a uniform loading. It was observed that the cracks become prominent and measurable at applied loads of 1N and above. Fig.4. shows representative micrographs of indentation marks and cracks associated with them at an applied load of 2N.

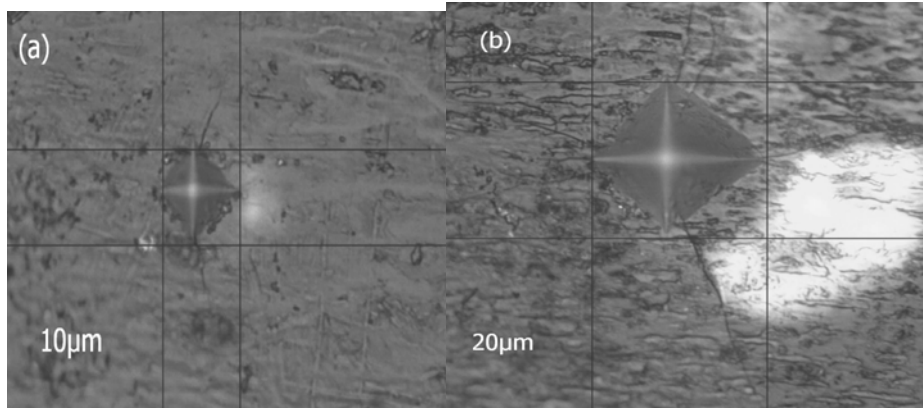


Fig. 4. Optical micrograph of indentation mark.

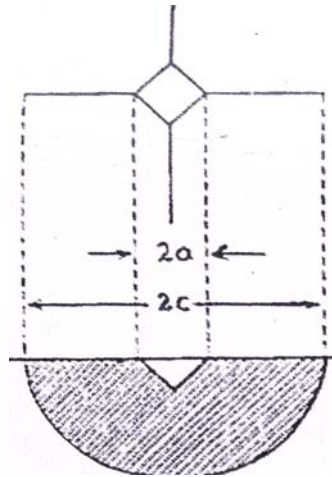


Fig. 5. Schematic diagram of measurement of crack length.

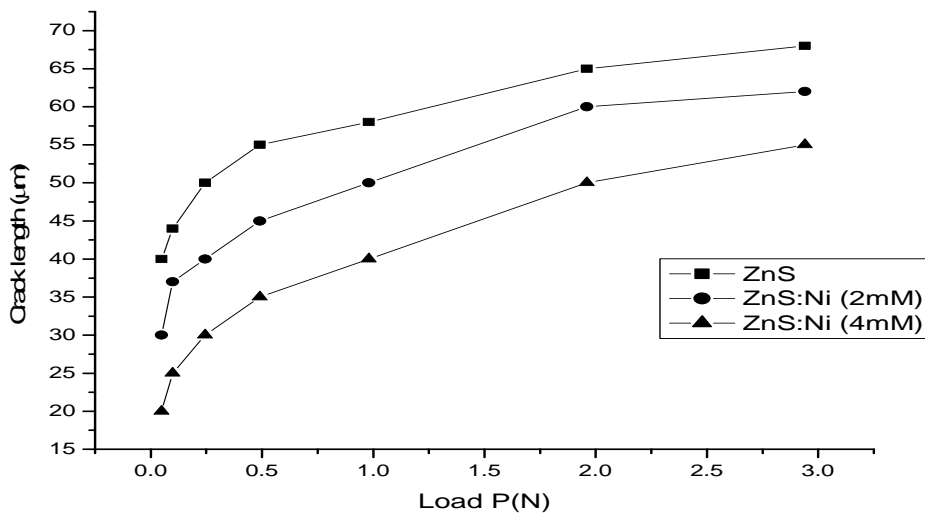


Fig. 6. Crack length vs. load

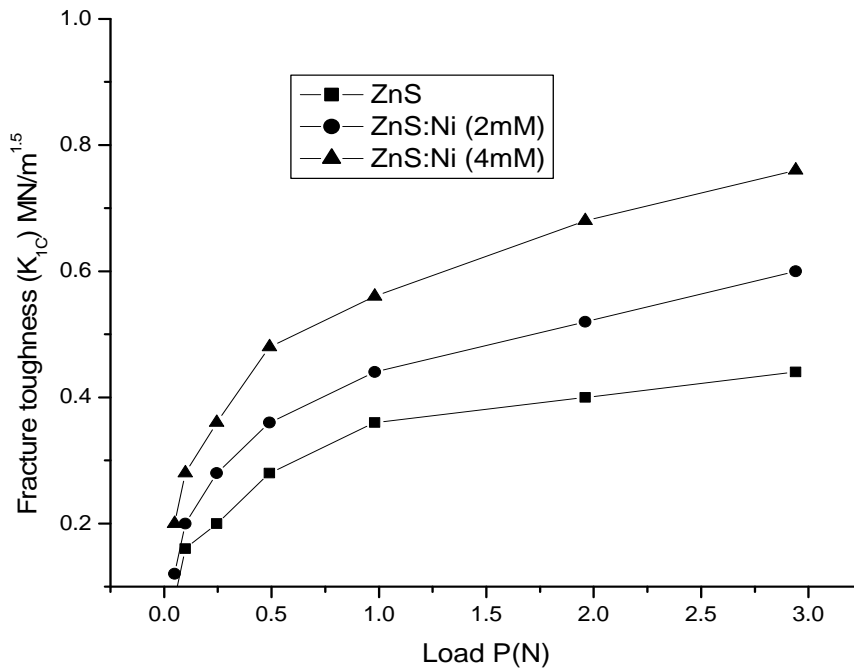


Fig. 7. Effect of load on fracture toughness.

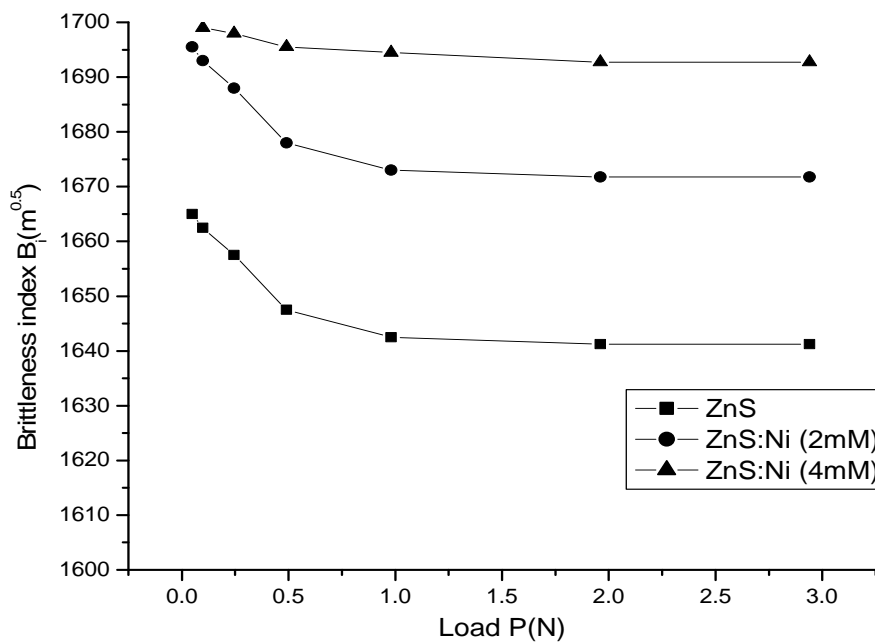


Fig. 8. Brittleness index vs. load.

For a material with well defined cracks, the resistance to the fracture indicates the fracture toughness of the material. The fracture toughness determines how much fracture stress is applied under uniform loading. The term toughness is also defined as the property of material by means of which it can absorb maximum energy before the fracture takes place. The fracture toughness is an important parameter for the selection of materials for application where the load exceeds yield point. A schematic diagram indicating the measurement of crack length is shown in fig.5. Generally, the fracture toughness (K_C) measured by the microindentation technique is expressed as [23]

$$K_C \Phi / H_v(a)^{1/2} = 0.15k(c/a)^{-3/2} \quad (7)$$

Where $a(=d/2)$ is half the diagonal length of the indentation impression and c is the crack length. By substituting $\Phi=3$ (ratio of hardness to yield strength which is generally as equal to 3) and $k=3.2$ and $H_v=1.8544P/d^2=0.47P/a^2$ the equation (7) reduces to

$$K_C = 0.0726/c^{3/2} \quad (8)$$

The crack length is found to increase with the increase in applied load (fig. 6). It is observed that the crack length at particular load decreases with the increase in Ni concentration. The load dependence on fracture toughness of different compositions of Ni modified ZnS nano crystals is shown in fig.7. Fracture toughness increases with increase in the load and attains saturation at higher loads in all compositions of Ni modified ZnS nano crystals. Fracture toughness at a given load is found to increase with an increase in Ni substitution. The equilibrium equation for materials having an internal stress σ_i is expressed as

$$[P/c^{3/2}]_{\sigma_i} = [[P/c^{3/2}]_{\sigma_0} [1 + 2 \sigma_i(c/\pi)/K_{IC}] \quad (9)$$

On substituting value of K_{IC} from equation gives a relation between fracture toughness and intrinsic fracture toughness (K_{IC}^0) as follows

$$K_{IC} = K_{IC}^0 + 2 \sigma_i(c/\pi)^{3/2} \quad (10)$$

The relation indicates that the internal stress can be derived from the slope of K_{IC} versus $c^{1/2}$ plot. Fig. 8. Shows the dependence of square root of crack length on fracture toughness of pure and Ni modified ZnS nano crystals. The lines drawn by linear fit suggest the slope decreasing with the increase in Ni content. This indicates that the internal stress decrease with increase in Ni substitution in the parent compound. This is consistent with the fact that the decrease in unit cell volume has been noticed with increase in Ni substitution [16].

Brittleness is an important property that affects the mechanical behaviour of a material and gives an idea about the fracture induced in a material without any appreciable deformation. The value of brittleness index B_i [24] is calculated using Equation:

$$B_i = H_v/K_c \quad (11)$$

Comparison of data on brittleness index of pure and Ni modified ZnS nano crystals leads to interesting results.

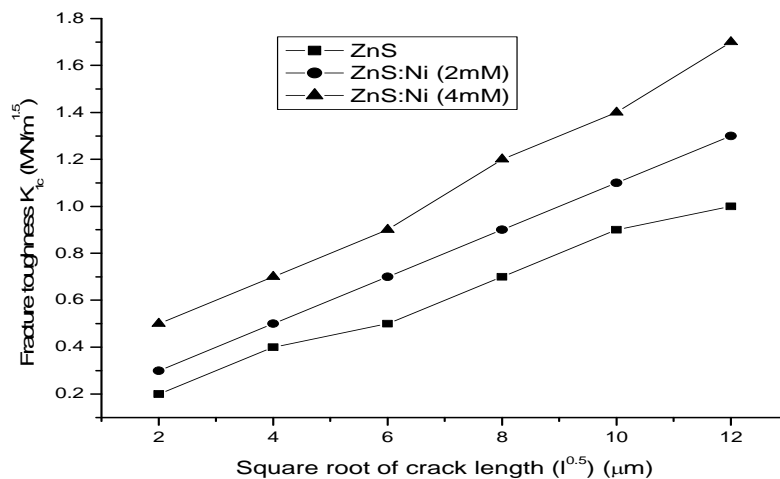


Fig. 9. Fracture toughness vs. crack length

The brittleness index shows decrease in its value at each load ranging from 0.049 to 3N on doping ZnS nano crystals. The dependence of brittleness index on load for pure and Ni modified ZnS nano crystals are reflected by Fig.8.

Table 1 data on microhardness measurements and analysis for various ZnS:Ni

Crystal	n_k	n_h	K_1 GN/m ²	K_2 GN/m ²	W(N)
x=0	1.69	1.99	5.66	2.26	0.045
x=0.2	1.65	1.98	4.23	1.77	0.041
x=0.4	1.64	1.96	3.66	1.52	0.036

4. Conclusions

In summary, the microhardness of pure ZnS and Ni modified ZnS decreases nonlinearly in the load range 0.049-2N and tends to attain saturation thereafter. Hardness becomes independent of load at loads greater than 2N upto the maximum (as taken in the present case) applied load 3N. Decrease in microhardness in low load region (0.049-2) is explained on the basis of Newtonian resultant pressure as proposed by Hay's and Kendall's law. Load independent values of microhardness as calculated on application of Hay's and Kendall's law is consistent with the saturated value of microhardness. A load independent value of microhardness is found to increase linearly with the increase in Ni substitution. Well defined and measurable cracks are associated with the indentation impression at a load of 1N and above. However at constant load, crack length decreases with increase in Ni substitution. The internal stress measured by microindentation technique decreases with increase in Ni substitution. This is due to the fact that the increase in Ni substitution decreases unit cell volume [16] which in turn decreases the internal stress.

Acknowledgements

The author is pleased to acknowledge Director Mr Mubashir, National Institute of Technology for his kind support and HOD metallurgical engineering department (NIT Srinagar) for providing experimental facilities. The author is also thankful to the principal (Prof. M.A.Mir) and Dr. Iqbal, GDC Handwara, J&K (Department of higher education) for his kind support during this research work.

References

- [1] D.J. Norris, N. Yao, F.T. Charnock, T.A. Kennedy, *Nano Lett.* **1**, 3 (2001).
- [2] W. Chen, J.-O. Malm, V. Zwiller, Y. Huang, S. Liu, R. Wallenberg, J.-O. Bovin, L. Samuelson, *Phys. Rev. B* **61**, 11021 (2000).
- [3] Y.L. Soo, Z.H. Ming, S.W. Huang, Y.H. Kao, R.N. Bhargava, D. Gallagher, *Phys. Rev. B* **50** 7602 (1994)
- [4] A. P. Alivisatos, *J. Phys. Chem.* **100**,13226 (1996).
- [5] R. Pool, *Science* **248**, 1186 (1990).
- [6] S. Chen, W. Liu, *Mater. Res. Bull.* **36**, 137 (2001)
- [7] L. Brus, *Applied Phys. A* **53**, 465 (1991)
- [8] S. C. Qu, W. H. Zhou, F. Q. Liu, N. F. Chen, and Z. G. Wang, H. Y. Pan, D. P. Yu, *Appl. Phys. Lett.* **80**, (2002).
- [9] A. Ishizumia, C.W. Whiteb, Y. Kanemitsu, *Physica E* **26**, 24 (2005).

- [10] V. L. Colvin, M. C. Schlamp, A. P. Alivisatos, *Nature* **370**, (1994).
- [11] P. Yang, M. Lu, D. Xu, D. Yuan, G. Zhou, *Appl. Phys. A* **73**, 455 (2001).
- [12] S. M. Liu, H. Q. Guo, Z. H. Zhang, F. Q. Liu and Z. G. Wang, *Chin. Phys. Lett.* **17**, 609 (2000).
- [13] D. D. Papakonstantinou, J. Huang, P. Lianos, *Journal of Materials Science-Letters* **17**, 1571 (1998), -1573.
- [14] S. J. Xu, S. J. Chua, B. Liu, L. M. Gan, C. H. Chew, Q. Q. Xu, *Appl. Phys. Lett.* **73**, 478 (1998).
- [15] T. Trindade, P. O. Brien, *J. Mater. Chem.* **6**, 343 (1996)
- [16] Arfat. Firdous, *European Jr. of Applied Physics*, (2010), in press
- [17] E.F. Bertaut, (*New York Academic*) 149 (1963).
- [18] H. Horner and C.M. Varma, *Phys. Rev. Lett.*, **20**, 845 (1958).
- [19] T. Yamaguchi and K. Tsushima, *Phys. Rev.*, **B8**, 5187(1973) .
- [20] J.K. Vassiliou et al., *Solid State Chem.*, **81**, 208 (1989).
- [21] J.B. Torrance et al., *Phys. Rev.*, **B45,14**, 8209 (1992).
- [22] O.M. Hemeda et al., *J. Thermal Analysis*, **38**, 2291 (1992).
- [23] E. Rezlescu, N. Rezlescu, P.D. Popa, L.Rezlescu and C. Pas, Nicu. *Phys. Stat. Sol. (a)* **162**, 673 (1997).
- [24] V.M. Goldschmidt, *Naturwissenscha_en*, **14**, 477(1926).

*Corresponding author: narfat2phy@gmail.com